Simplified Modified Compression Field Theory for Calculating Shear Strength of Reinforced Concrete Elements

by Evan C. Bentz, Frank J. Vecchio, and Michael P. Collins

This paper summarizes the results of over 100 pure shear tests on reinforced concrete panels. The ACI approach for predicting shear strength as the sum of a diagonal cracking load and a 45-degree truss model predicts the strength of these panels poorly, with an average experimental-over-predicted shear strength ratio of 1.40 with a coefficient of variation of 46.7%. Based on a subset of these experiments, an expressive but relatively complex analysis method called the modified compression field theory (MCFT) was developed in the 1980s that is able to predict full load deformation relationships. This theory can predict the shear strength of these panels with an average shear strength ratio of 1.01 and a coefficient of variation (COV) of only 12.2%. This paper presents a new simplified analysis method that can predict the strength of these panels in a method suitable for "back of the envelope" calculations. This new method gives an average shear strength ratio of 1.11 with a COV of 13.0%. The application of this new simplified method to panels is demonstrated with numerical examples.

Keywords: reinforced concrete; safety; shear; strength.

INTRODUCTION

Even though the behavior of reinforced concrete in shear has been studied for more than 100 years, the problem of determining the shear strength of reinforced concrete beams remains open to discussion. Thus, the shear strengths predicted by different current design codes[1-5] for a particular beam section can vary by factors of more than 2. In contrast, the flexural strengths predicted by these same codes are unlikely to vary by more than 10%. For flexure, the plane sections hypothesis forms the basis of a universally accepted, simple, rational theory for predicting flexural strength. In addition, simple experiments can be performed on reinforced concrete beams subjected to pure flexure and the clear results from such tests have been used to improve the theory. In shear, there is no agreed basis for a rational theory, and experiments cannot be conducted on reinforced concrete beams subjected to pure shear.

A traditional shear test on a reinforced concrete beam is depicted in Fig. 1(a). The region of the beam between the two point loads is subjected to pure flexure, whereas the shear spans of the beam are subjected to constant shear and linearly varying moment. Because the behavior of this member is changing from section to section along the shear span, it is difficult to use the results of such a test to develop a general theory for shear behavior. Thus, if a relationship is sought between the magnitude of the shear force and the strains in the stirrups, it will be found that the strains are different for every stirrup and also differ over the height of each stirrup. In addition, the high net vertical compressive stresses f_z, called "clamping stresses," near the point loads and reactions cause stirrup strains in these locations to be close to zero.

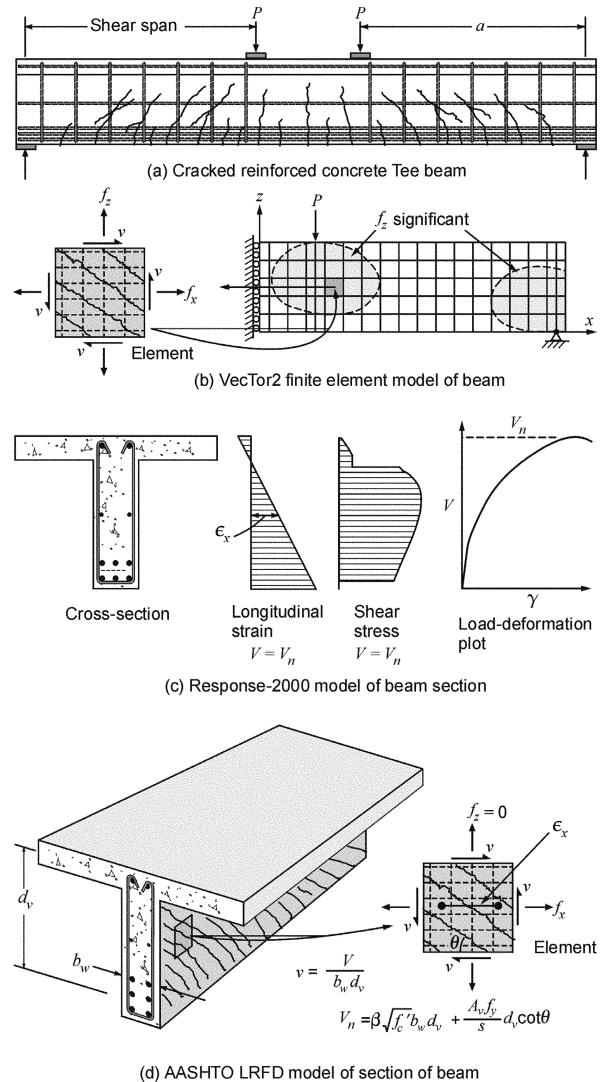Fig. 1—Predicting shear strength of reinforced concrete beams.

The modified compression field theory[6] (MCFT) was developed by observing the response of a large number of reinforced concrete elements loaded in pure shear or in shear combined with axial stress. While such tests were more difficult to perform, they gave experimental results that clearly illustrated the fundamental behavior of reinforced concrete in shear.

ACI member **Evan C. Bentz** *is an Associate Professor of Civil Engineering at the University of Toronto, Toronto, Ontario, Canada. He is a member of ACI Committee 365, Service Life Prediction, and Joint ACI-ASCE Committee 445, Shear and Torsion. His research interests include the mechanics of reinforced concrete, service-life modeling, and the creation of practical tools that transfer reinforced concrete research into the engineering community.*

Frank J. Vecchio, *FACI, is a Professor in the Department of Civil Engineering, University of Toronto. He is a member of Joint ACI-ASCE Committees 441, Reinforced Concrete Columns, and 447, Finite Element Analysis of Reinforced Concrete Structures. His research interests include nonlinear analysis and design of concrete structures; constitutive modeling; and assessment, repair, and rehabilitation of structures.*

Michael P. Collins, *FACI, is University Professor and Bahen-Tanenbaum Professor of Civil Engineering at the University of Toronto. He is a member of ACI Committee 318, Structural Concrete Building Code, and Joint ACI-ASCE Committee 445, Shear and Torsion. His research interests include development of rational and consistent shear design specifications for structural concrete applications.*

The problem addressed by the MCFT is to predict the relationships between the axial and shear stresses applied to a membrane element, such as that shown in Fig. 1(b), and the resulting axial and shear strains. If the theory can accurately predict the behavior of such an element, it can be used as the basis for a range of analytical models. The most accurate, but most complex, of these models involves representing the structure as an array of biaxial elements and then conducting a nonlinear finite element analysis[7] using a computer program[8] (refer to Fig.1(b)). This model gives accurate results both in flexural regions and in disturbed regions where high clamping stresses can significantly increase shear strength. If one assumes that plane sections remain plane and that the vertical clamping stresses are negligibly small, one can model one section of a beam as a vertical stack of biaxial elements. This is the basis of program Response-2000,[9] which is capable of predicting the shear stress distribution over the height of the beam and the shear force-shear deformation relationship of the section (Fig. 1(c)). Finally, reasonably simple expressions for the shear strength of a section can be derived if just one biaxial element within the web of the section is considered and the shear stress is assumed to remain constant over the depth of the web. This is the basis of the sectional design model for shear[10] included in the AASHTO LRFD Bridge Design Specifications[2] (Fig. 1(d)).

In the AASHTO LRFD shear design method, the shear strength of a section is a function of the two parameters β and θ. The inclination θ of the diagonal compressive stresses in the web, and the factor for tensile stresses in the cracked concrete, β, both depend on the longitudinal straining of the web, ε_x. For members without transverse reinforcement, β and θ values calculated from the MCFT are given as functions of ε_x and the crack spacing s_{xe} in a table. A separate table is given for the β and θ values for members with transverse reinforcement.

Shear design procedures should be simple to understand and to use not only for ease of calculation but, more critically, for ease of comprehension. The engineer should be able to give physical significance to the parameters being calculated and to understand why they are important. If the procedures are simple enough, an experienced engineer should be able to perform at least preliminary calculations on the "back of an envelope." While the use of the required tables in the AASHTO LRFD shear design method is straightforward, it is not possible to remember the values in the tables for "back of the envelope" calculations. Further, many engineers prefer simple equations to tables because they give a continuous range of values and are more convenient for spreadsheet calculations. In this paper, simple equations for β and θ will be determined from the basic expressions of the MCFT. In addition, the paper will summarize the observed shear strengths of 102 reinforced concrete elements tested in shear and show how, by the use of the simple equations, the strength of these elements can be predicted accurately.

RESEARCH SIGNIFICANCE

The research reported in this paper has resulted in a significant simplification of the MCFT. It is shown that this simplified

Equilibrium:
Average Stresses:

$$f_x = \rho_x f_{sx} + f_1 - v \cot\theta \tag{1}$$

$$f_z = \rho_z f_{sz} + f_1 - v \tan\theta \tag{2}$$

$$v = (f_1 + f_2)/(\tan\theta + \cot\theta) \tag{3}$$

Stresses at Cracks:

$$f_{sxcr} = (f_x + v \cot\theta + v_{ci} \cot\theta)/\rho_x \tag{4}$$

$$f_{szcr} = (f_z + v \tan\theta - v_{ci} \tan\theta)/\rho_z \tag{5}$$

Geometric Conditions:
Average Strains:

$$\tan^2\theta = \frac{\epsilon_x + \epsilon_2}{\epsilon_z + \epsilon_2} \tag{6}$$

$$\epsilon_1 = \epsilon_x + \epsilon_z + \epsilon_2 \tag{7}$$

$$\gamma_{xz} = 2(\epsilon_x + \epsilon_2)\cot\theta \tag{8}$$

Crack Widths:

$$w = s_\theta \epsilon_1 \tag{9}$$

$$s_\theta = 1 / \left(\frac{\sin\theta}{s_x} + \frac{\cos\theta}{s_z} \right) \tag{10}$$

Stress-Strain Relationships:
Reinforcement:

$$f_{sx} = E_s \epsilon_x \le f_{yx} \tag{11}$$

$$f_{sz} = E_s \epsilon_z \le f_{yz} \tag{12}$$

Concrete:

$$f_2 = \frac{f_c'}{0.8 + 170\epsilon_1}\left[2\frac{\epsilon_2}{\epsilon_c'} - \left(\frac{\epsilon_2}{\epsilon_c'}\right)^2 \right] \tag{13}$$

$$f_1 = 0.33\sqrt{f_c'}/\left(1 + \sqrt{500\,\epsilon_1}\right) \text{ MPa} \tag{14}$$

Shear Stress on Crack:

$$v_{ci} \le \frac{0.18\sqrt{f_c'}}{0.31 + \frac{24\,w}{a_g + 16}} \text{ MPa, mm} \tag{15}$$
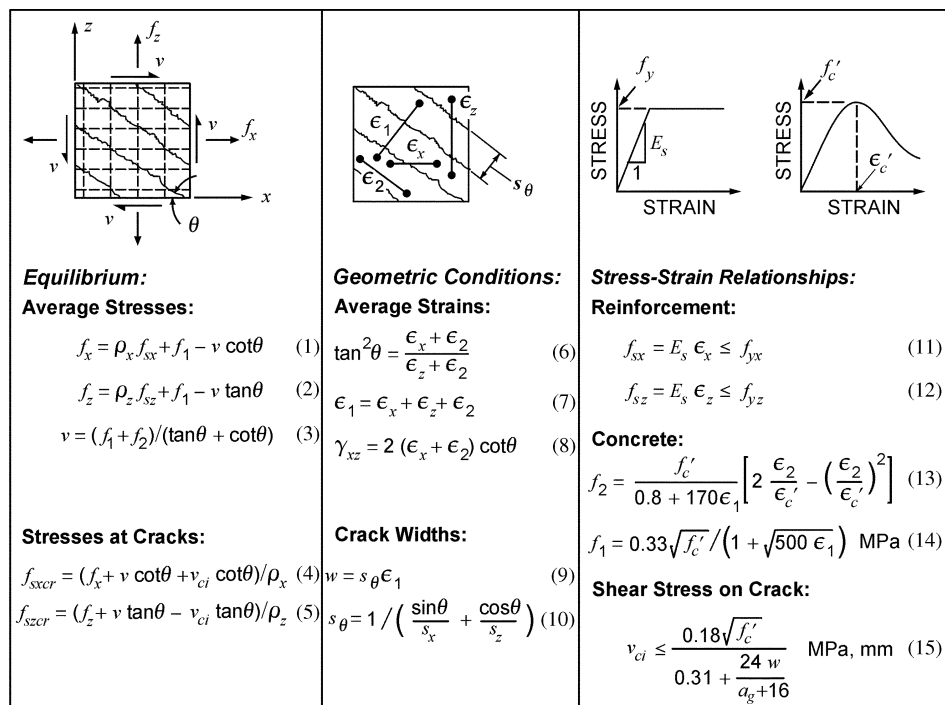
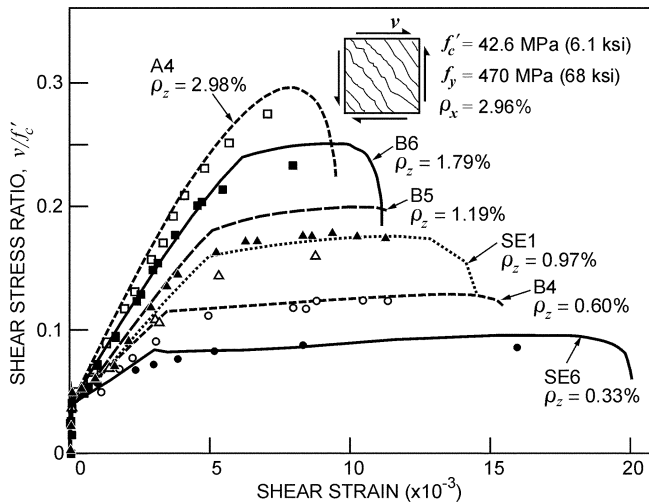*Fig. 2—Equations of modified compression field theory.*

Fig. 3—Comparison of predicted and observed shear stress-shear strain response of six elements.

MCFT is capable of predicting the shear strength of a wide range of reinforced concrete elements with almost the same accuracy as the full theory. The expressions developed in the paper can form the basis of a simple, general, and accurate shear design method for reinforced concrete members.

BACKGROUND TO MCFT

The original shear design procedure[11,12] for reinforced concrete, which was developed more than 100 years ago, assumed that cracked concrete in the web of a beam resisted shear stress v only by diagonal compressive stresses f_2 and that these stresses were inclined at an angle of 45 degrees to the longitudinal axis of the member. The diagonal compressive stresses push apart the flanges of the beam causing tension in the stirrups, which are responsible for holding together the two flanges. After the stirrups yield, the beam is predicted to be capable of resisting a shear stress of $\rho_z f_y$, where ρ_z is the ratio of the stirrup area to the web area, $\rho_z = A_v/(b_w s)$, and f_y is the yield stress of the stirrups. Because the 45-degree truss model ignores any contributions of the tensile strength of the concrete, it can give very conservative estimates of shear strength for members with small amounts of stirrups. Because of this, for the last 40 years, the ACI specifications[1,13] have taken the shear strength of the web of a beam as $\rho_z f_y + v_c$ where the concrete contribution v_c is taken as the shear stress at which diagonal cracks form, v_{cr}. Axial tension reduces v_{cr} and, hence, is predicted to decrease shear strength whereas axial compression or prestressing increases v_{cr} and, hence, is predicted to increase shear strength.

During the 1970s and 1980s, European researchers focused attention on the fact that, in general, θ is not 45 degrees. From a truss model with diagonals inclined at an angle of θ, the shear stress capacity of a web is predicted to be $\rho_z f_y \cot\theta$. The difficulty is to determine an appropriate value of θ. Models[14,15] based on the theory of plasticity were developed allowed the engineer to select the value of θ. Because concrete shear failures are brittle, however, it was necessary to place somewhat arbitrary limits on θ (for example, $\theta > 30$ degrees) and on f_2 (for example, $f_2 < 0.6f_c'$ to avoid unsafe predictions.

The development of the compression field theory[16,17] (CFT) was a significant step toward a more rational theory for shear. Unlike traditional models, the theory uses the strain conditions in the web to determine the inclination θ of

the diagonal compressive stresses. The relationship is that $\tan^2\theta = (\varepsilon_x + \varepsilon_2)/(\varepsilon_z + \varepsilon_2)$, where ε_x is the longitudinal strain in the web (tensile positive, compressive negative), ε_z is the transverse tensile strain in the web, and ε_2 is the diagonal compressive strain. Because ε_x is usually much smaller than ε_z, the angle θ can be considerably less than 45 degrees, which increases the predicted shear strength of the web. Prestressing or axial compression can significantly reduce ε_x and, hence, is predicted to lower the angle θ and thus increase shear strength.

To study the relationship between the diagonal compressive stress f_2 and the diagonal compressive strain ε_2, Vecchio and Collins[18] tested 30 reinforced concrete elements under biaxial stresses in an innovative testing machine. They found that f_2 is a function not only of ε_2 but also of the coexisting principal tensile strain ε_1. They also found that even after extensive diagonal cracking, tensile stresses still existed in the concrete between the cracks. Combined with shear stresses on the crack faces, v_{ci}, these tensile stresses increased the ability of the cracked concrete to resist shear. When the CFT relationships were modified to account for the average principal tensile stresses in the cracked concrete, f_1, the equilibrium, geometric, and constitutive relationships of the MCFT[6] were obtained. Figure 2 gives the 15 equations used[19] in the MCFT. Note that, in this context, average strains refer to strains measured over base lengths at least equal to the crack spacing. Average stresses are calculated considering effects both at and between the cracks and are distinct from stresses calculated at cracks.

Solving the equations of the MCFT given in Fig. 2 is, of course, very tedious if done by hand, but is quite straightforward with an appropriate computer program. Membrane-2000[9] is such a program and its ability to predict the load-deformation response of reinforced concrete membrane elements is demonstrated in Fig. 3. The six elements shown in this figure all contained approximately 3% of longitudinal reinforcement and were loaded in pure shear. The SE elements were tested at the University of Toronto[20,21] while the A and B elements were tested at the University of Houston.[22] Note that as the amount of transverse reinforcement was increased, the post-cracking shear stiffness and the shear strength of the elements increased, but the ductility of the elements decreased. It can be seen that there is excellent agreement between the lines representing the response predicted by the MCFT and the points showing the measured response.

DERIVATION OF SIMPLIFIED MCFT

The simplified version of the MCFT is a procedure by which the shear strength of an element can be conveniently computed. Because the element will be used to model a section in the flexural region of a beam, it is assumed that the clamping stresses f_z will be negligibly small (Fig. 1(d)). For the transverse reinforcement to yield at failure, ε_z will need to be greater than approximately 0.002, while to crush the concrete, ε_2 will need to be approximately 0.002. If ε_x is also equal to 0.002 at failure, Eq. (3), (6), (7), (13), and (14) predict that the maximum shear stress will be approximately $0.28f_c'$, whereas for very low values of ε_x, the shear stress at failure is predicted to reach approximately $0.32f_c'$. As a conservative simplification, it will be assumed that if failure occurs before yielding of the transverse reinforcement, the failure shear stress will be $0.25f_c'$. For failures occurring below this shear stress level, it will be assumed that at failure both f_{sz}

and f_{szcr} are equal to the yield stress of the transverse reinforcement, which will be called f_y.

Equation (5) given in Fig. 2 can be derived by considering the sum of the forces in the z-direction for the free body diagram shown in Fig. 4. For $f_z = 0$ and $f_{szcr} = f_y$, this equation can be rearranged to give

$$v = v_{ci} + \rho_z f_y \cot \theta \qquad (16)$$

In a similar fashion, Eq. (2) can be rearranged to give

$$v = f_1 \cot \theta + \rho_z f_y \cot \theta \qquad (17)$$

Both of these equations can be expressed as

$$v = v_c + v_s = \beta \sqrt{f'_c} + \rho_z f_y \cot \theta \qquad (18)$$

From Eq. (14), (17), and (18), the value of β is given by

$$\beta = \frac{0.33 \cot \theta}{1 + \sqrt{500 \varepsilon_1}} \qquad (19)$$

Similarly from Eq. (15), (16), and (18), the value of β must satisfy

$$\beta \leq \frac{0.18}{0.31 + 24w(a_g + 16)} \qquad (20)$$

The crack width w is calculated as the product of the crack spacing s_θ and the principal tensile strain ε_1. The term a_g represents the maximum coarse aggregate size in mm. The crack spacing depends on the crack control characteristics of the x-direction reinforcement, which is expressed by the parameter s_x, and the crack control characteristics of the z-direction reinforcement, which is expressed by s_z (Eq. (10)). As a simplification, s_x can be taken as the vertical distance between bars aligned in the x-direction and s_z can be taken as the horizontal spacing between vertical bars aligned in the z-direction. For elements with no transverse reinforcement, s_θ will equal $s_x / \sin \theta$ and Eq. (20) can be expressed as

$$\beta \leq \frac{0.18}{0.31 + 0.686 s_{xe} \varepsilon_1 / \sin \theta} \qquad (21)$$

where

$$s_{xe} = \frac{35 s_x}{a_g + 16} \qquad (22)$$

If in.-lb units are being used, the 0.18 in Eq. (21) should be replaced by 2.17, while the 35 and 16 in Eq. (22) should be replaced with 1.38 and 0.63, respectively. In elements made from high-strength concrete ($f'_c > 70$ MPa [10,000 psi]), cracks tend to break through the aggregate rather than passing around them; in such cases, a_g should be taken as zero.

For members without transverse reinforcement, the highest value of β and, hence, the maximum post-cracking shear capacity, will occur when Eq. (19) and (21) give the
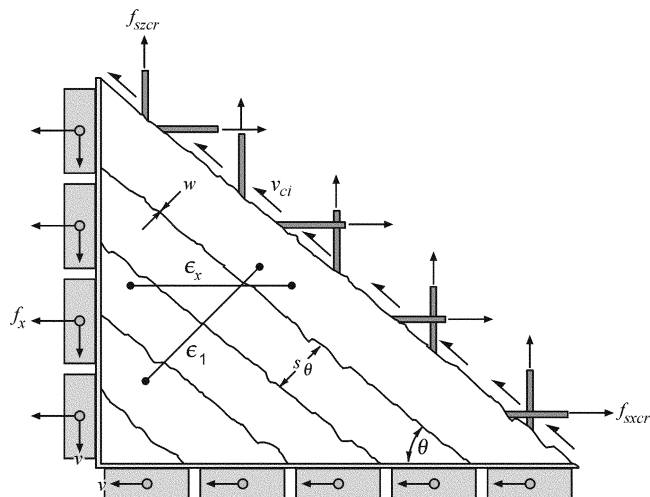
Fig. 4—Transmission of forces across cracks.
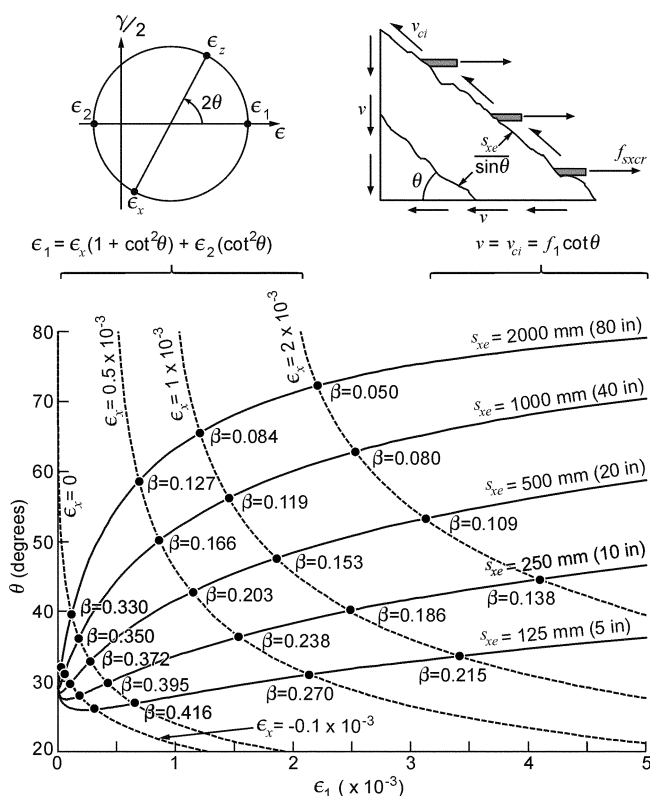
Fig. 5—Determination of beta and theta values for elements not containing transverse reinforcement.

same value for β.[23] This requirement results in the following equation

$$\tan \theta = \frac{0.568 + 1.258 s_{xe} \varepsilon_1 / \sin \theta}{1 + \sqrt{500 \varepsilon_1}} \qquad (23)$$

The manner in which this equation relates the inclination θ of the diagonal compressive stresses to the principal tensile strain ε_1 for different values of the crack spacing parameter s_{xe} is shown in Fig. 5.

To relate the longitudinal strain ε_x to ε_1, Eq. (6) and (7) can be rearranged to give

Fig. 6—Comparison of values for theta and beta given by simple equations with values determined from MCFT for elements without transverse reinforcement.

$$\varepsilon_1 = \varepsilon_x(1 + \cot^2 \theta) + \varepsilon_2 \cot^2 \theta \qquad (24)$$

The principal compressive strain ε_2 depends on the principal compressive stress f_2. When ρ_z and f_z are zero, Eq. (2) and (3) can be rearranged to give

$$f_2 = f_1 \cot^2 \theta \qquad (25)$$

Because the compressive stresses for these elements will be small, it is sufficiently accurate to assume that ε_2 equals f_2/E_c, and that E_c can be taken as $4950\sqrt{f_c'}$ in MPa units. Equation (24) then becomes

$$\varepsilon_1 = \varepsilon_x(1 + \cot^2 \theta) + \frac{\cot^4 \theta}{15,000(1 + \sqrt{500\varepsilon_1})} \qquad (26)$$

The manner in which this geometric equation relates ε_1 and θ for different values of ε_x is shown in Fig. 5. The intersection points of the lines representing given values of ε_x and s_{xe} define the values of θ and ε_1, which will simultaneously solve both Eq. (23) and (26). The corresponding

values of β, which can be found from Eq. (19), are shown in Fig. 5. It can be seen that as the crack spacing s_{xe} increases, the values of β and, hence, the shear strengths, decrease. The observed fact is that large reinforced beams that do not contain transverse reinforcement fail at lower shear stresses than geometrically similar smaller beams.[24-26] is known as the size effect in shear. It is of interest that the predictions of the MCFT (for example, that the size effect is related to the distance between the layers of longitudinal reinforcement rather than the overall size of the element) agree well with the results of the extensive experimental studies[27] on size effect done in the years since the theory was first formulated.

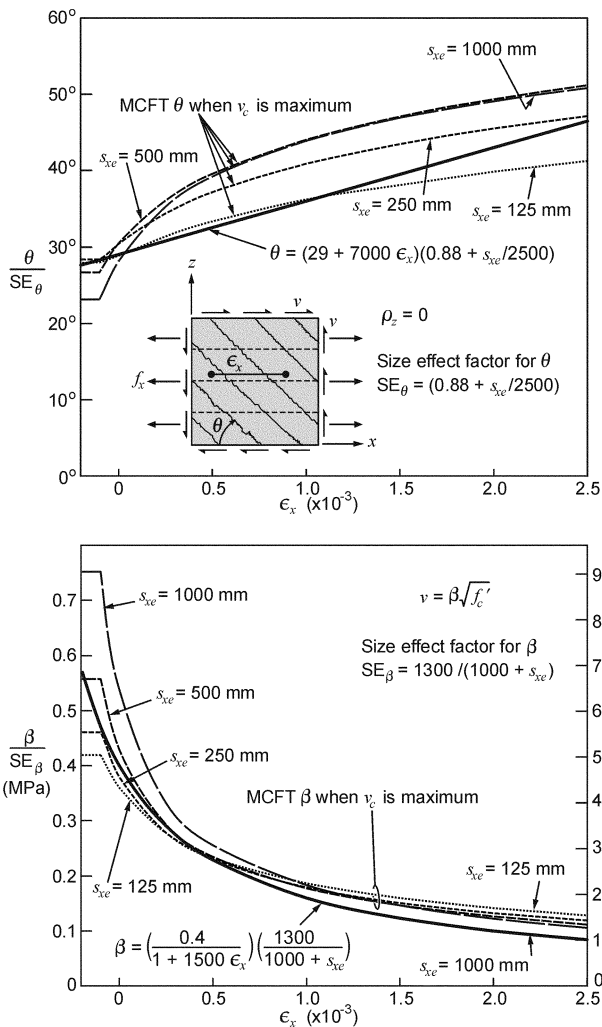The MCFT β values for elements without transverse reinforcement depend on both the longitudinal strain ε_x and the crack spacing parameter s_{xe}. The authors refer to these two effects as the "strain effect factor" and the "size effect factor." The two factors are not really independent, but in the simplified version of the MCFT, this interdependence of the two factors is ignored and it is assumed that β can be taken as simply the product of a strain factor and a size factor. Equation (27) is the suggested expression for β. The β-values given by this equation are compared to the values from the MCFT in Fig. 6. It can be seen that for all but very small values of ε_x combined with small values of s_{xe}, the simple equation gives values that are somewhat conservative.

$$\beta = \frac{0.4}{1 + 1500\varepsilon_x} \cdot \frac{1300}{1000 + s_{xe}} \qquad (27)$$

Equation (27) is to be used with a concrete strength, in MPa, and s_{xe}, in millimeters. If in.-lb units are used for s_{xe}, the 1300 in Eq. (27) becomes 51 and the 1000 becomes 39. Further, for use with concrete strengths in psi, the 0.4 becomes 4.8.

The simplified MCFT uses the following expression for the angle of inclination θ

$$\theta = (29 \deg + 7000\varepsilon_x)\left(0.88 + \frac{s_{xe}}{2500}\right) \le 75 \deg \qquad (28)$$

If in.-lb units are used for s_{xe}, the 2500 in Eq. (28) becomes 100. Equation (28) again assumes that the relationship is simply the product of a strain factor and a size factor. The angles predicted by this equation are compared with those derived from the MCFT in Fig. 6. For members without transverse reinforcement, it is conservative to underestimate θ, as this will increase the calculated stress in the longitudinal reinforcement. It can be seen from Fig. 6 that the θ-values given by Eq. (28) are conservative for nearly all of the different combinations of values of ε_x and s_{xe}.

As elements containing both longitudinal and transverse reinforcement approach shear failure, the MCFT predicts that there can be a substantial change in the relative magnitudes of v_c and v_s. Typically, after yielding of the transverse reinforcement, the angle θ will become smaller, causing v_s to increase. At the same time, the resulting large increase in ε_1 will decrease v_c. A substantial decrease in θ will also cause a major increase in the stress in the longitudinal reinforcement. A conservative approach for determining θ for the simplified MCFT is to consider the value of θ at which the MCFT predicts that v_c has its maximum contribution to the strength. Also note that it would be convenient if the

same expressions could be used both for members with and for members without transverse reinforcement. Hence, Fig. 7 compares the values of θ associated with maximum v_c with those predicted by Eq. (28). It can be seen that the agreement is reasonable. Note that, for these elements, a high value of θ is conservative as it decreases v_s. Also note that for elements containing both longitudinal and transverse reinforcement, the spacing of the diagonal cracks will typically be less than 300 mm (12 in.) and, hence, it is conservative to take s_{xe} as 300 mm (12 in.) in Eq. (27) and (28). Figure 7 also compares the corresponding β-values predicted by the MCFT for these elements with the values given by Eq. (27). It can be seen that while the β-values predicted by the simple equation are conservative over much of the range of possible ε_x-values, they are somewhat unconservative for very low values of ε_x. In this range, however, the unconservative estimate for β will be partly compensated by the conservative estimate for θ.

SIMPLIFIED MCFT STRENGTH PREDICTIONS FOR ELEMENTS

To illustrate how the simplified MCFT can be used to predict shear strength, consider the series of elements whose load-deformation plots are shown in Fig. 3. It will be recalled that these elements were loaded in pure shear and all contained approximately 3% of longitudinal reinforcement. It is desired to predict how the shear strength will increase as the amount of transverse reinforcement is increased. As an example, the case where the amount of transverse reinforcement is such that $\rho_z f_y$ equals 2 MPa (290 psi) is used. The calculations are begun by estimating the value of ε_x corresponding to the maximum capacity of the element. Thus, one might assume ε_x will be 1.0×10^{-3}. Using the average s_{xe} value for these elements, which is 158 mm (6.2 in.), Eq. (27) and (28) then predict that β equals 0.1796 and θ equals 34.0 degrees. The average concrete strength is 42.6 MPa (6180 psi) and Eq. (18) then predicts that the shear strength of the element will equal

$$v = v_c + v_s = 1.172 + 2.97 = 4.14 \text{ MPa (600 psi)}$$

If the longitudinal reinforcement is not yielding, Eq. (1) and (11) can be used to determine the value of longitudinal strain ε_x, which will correspond to this shear stress. As the applied axial stress f_x is zero and, as f_1 can be expressed as $v_c/\cot\theta$, these equations give

$$\varepsilon_x = \frac{f_{sx}}{E_s} = \frac{v \cot\theta - v_c/\cot\theta}{E_s \rho_x} \tag{29}$$

$$= \frac{4.14 \cot(34.0 \text{ deg}) - 1.172/\cot(34.0 \text{ deg})}{200,000 \cdot 0.0296} = 0.90 \times 10^{-3}$$

As 0.90×10^{-3} does not equal the assumed value of 1.0×10^{-3}, a new estimate of ε_x needs to be made and the calculations repeated. Convergence is reached when $\varepsilon_x = 0.939 \times 10^{-3}$. For this value of longitudinal strain, $v_c = 1.217$ MPa (176 psi), $\theta = 33.6$ degrees, and the failure shear v is predicted to be 4.23 MPa (613 psi). Note that this stress is below the $0.25f_c'$ limit and, hence, the assumption that the transverse reinforcement is yielding at failure is appropriate.
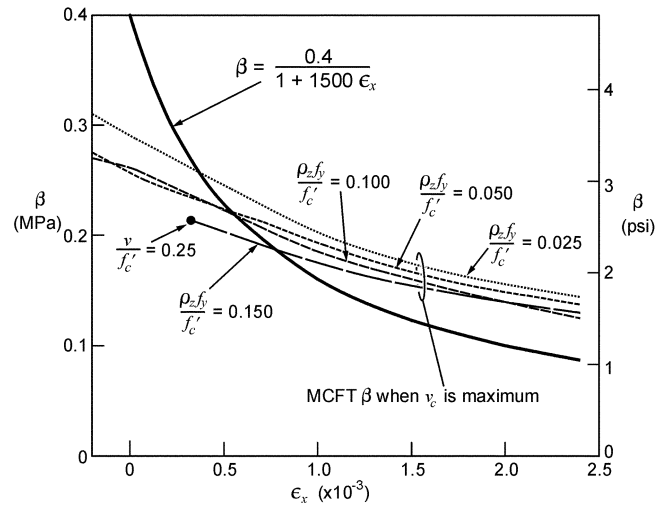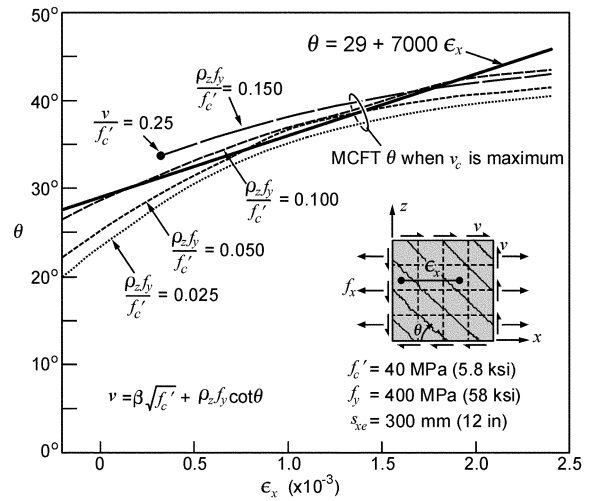
Fig. 7—Comparison of values for theta and beta given by simple equations with values determined from MCFT for elements with transverse reinforcement.

It remains to be checked that the longitudinal reinforcement can transmit the required stresses across the cracks without exceeding its yield stress. Because $f_x = 0$ and $v_{ci} = v_c$, Eq. (4) can be rearranged to give

$$f_{sxcr} = \frac{(v + v_c)\cot\theta}{\rho_x} \tag{30}$$

$$= \frac{(4.23 + 1.27)\cot(33.6 \text{ deg})}{0.0296} = 277 \text{ MPa (40.2 ksi)}$$

As this stress is less than the yield stress of the longitudinal reinforcement, the x-direction reinforcement is predicted not to yield at the cracks and, hence, the calculations for this element are complete.

Repeating the calculations for different values of $\rho_z f_y$ produced the values plotted in Fig. 8 as the line labeled "Simplified MCFT." Note that for this case when $\rho_z f_y/f_c'$ exceeds 0.200, the predicted shear capacity will be governed by the assumed upper limit on the shear strength of $0.25f_c'$. Also shown in Fig. 8 are the capacities predicted from program Membrane-2000, which implements the full MCFT and the shear strengths determined from the experiments. It
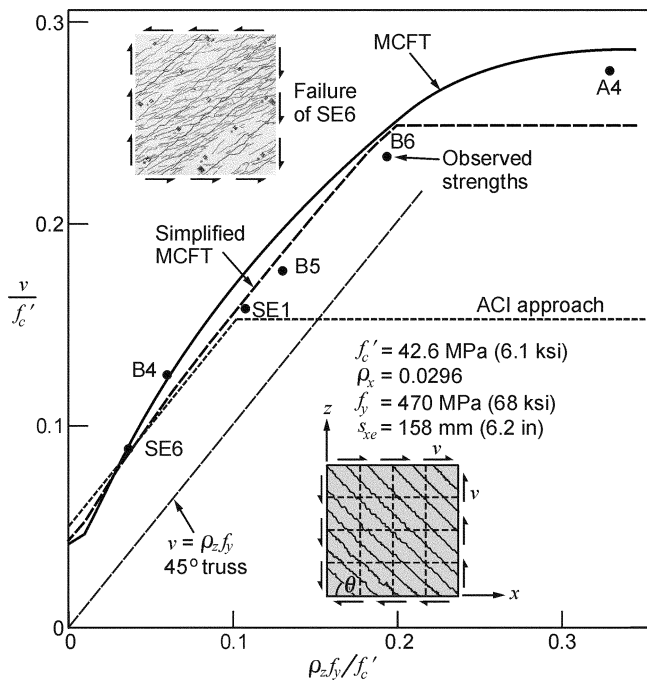
Fig. 8—Influence of amount of transverse reinforcement on shear strength of elements containing 2.96% of longitudinal reinforcement.
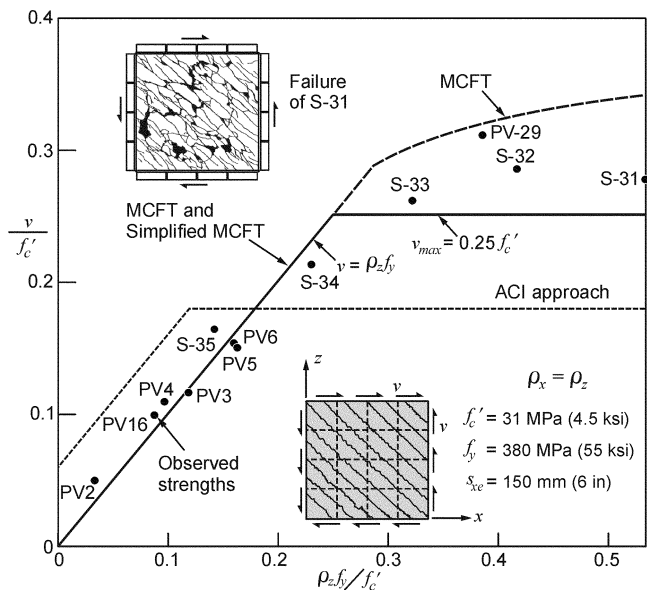
Fig. 9—Influence of amount of reinforcement on shear strength of elements containing equal amounts of longitudinal and transverse reinforcement.

can be seen that, for these elements, the predictions of the simplified MCFT are close to those of the MCFT and agree well with the experimental results. As expected, the predictions of the 45-degree truss model are very conservative. However, if the ACI approach of taking the shear capacity as the sum of the diagonal cracking shear, shown at $0.33\sqrt{f'_c}$ ($4\sqrt{f'_c}$ in psi units) in Fig. 8, and the 45-degree truss value is followed, accurate estimates of the shear capacities are obtained. In the ACI approach, v_s is limited to a shear stress of $0.66\sqrt{f'_c}$ ($8\sqrt{f'_c}$ in psi units), which results in a maximum predicted v/f'_c ratio of 0.153. It can be seen from Fig. 8 that this is a very conservative upper limit on shear capacity.

The elements in Fig. 8 all contained a substantial amount of longitudinal reinforcement and, hence, yielding of this x-direction reinforcement did not govern the shear strengths predicted by the simplified MCFT. To illustrate how yielding of the longitudinal reinforcement influences shear strength, a series of elements for which the amount of longitudinal reinforcement equals the amount of transverse reinforcement is considered. How the shear strength of these elements is predicted to increase as the amount of reinforcement increases will be determined (Fig. 9). The PV elements shown in this figure were tested by Vecchio and Collins,[6] whereas the S elements were tested by Yamaguchi et al.[28] As an example of calculating the strength of these elements, take the case when ρ_z and ρ_x are both equal to 0.79%, which corresponds to $\rho_z f_y = 3$ MPa (435 psi). As the x reinforcement will yield, ε_x will be greater than the yield strain, which is 1.90×10^{-3}, and Eq. (29) will not be applicable. To start the calculations, assume that ε_x equals 3.0×10^{-3}. Using the average s_{xe} value for these elements, which is 150 mm (6 in.), Eq. (27) and (28) predict that $\beta = 0.0822$ and $\theta = 47.0$ degrees. For a concrete strength of 31 MPa (4500 psi), the predicted shear strength from Eq. (18) then becomes

$$v = v_c + v_s = 0.0822\sqrt{31} + 3.00\cot(47.0 \text{ deg})$$

$$= 0.458 + 2.794 = 3.251 \text{ MPa (471 psi)}$$

Equation (30) can then be used to find f_{sxcr}

$$f_{sxcr} = \frac{(3.251 + 0.458)\cot(47.0 \text{ deg})}{0.0079}$$

$$= 438 \text{ MPa (63.5 ksi)}$$

As this predicted value of reinforcement stress exceeds the yield stress for this steel, which is 380 MPa (55.1 ksi), the assumed value of ε_x is not correct. Increasing ε_x will decrease the calculated value of f_{sxcr} and it will be found that ε_x must be increased to 3.30×10^{-3} before f_{sxcr} is reduced to the yield stress. At this value of longitudinal strain, the predicted shear strength of the element is 3.03 MPa (439 psi).

Repeating the aforementioned calculations for different amounts of reinforcement produced the values plotted in Fig. 9 as the line labeled "Simplified MCFT." Note that the predicted shear strengths for these elements with equal reinforcement in the x- and y-directions are essentially equal to $\rho_z f_y$, until $\rho_z f_y/f'_c$ reaches 0.25. The predictions from program Membrane-2000 for the shear strength of these elements is shown in Fig. 9 by the line labeled "MCFT." For the elements where the reinforcement yields at failure the predictions from the Simplified MCFT are essentially identical to those from the MCFT, and both are equal to those from the 45-degree truss model. Further, all three models agree well with the experimental results. For such elements with equal x and y reinforcement, it is unconservative to follow the ACI approach of estimating failure shear by adding the diagonal cracking shear to the 45-degree truss prediction.

As a final example of using the Simplified MCFT for predicting the shear strength of elements, consider a series tested by Bhide and Collins.[29,30] As shown in Fig. 10, these

specimens contained 2.20% of reinforcement in the *x*-direction, no reinforcement in the *z*-direction, and were loaded under different combinations of shear and uniaxial tension. The question being addressed by these tests was "how does magnitude of tension influence shear capacity?" Once again, the calculations start by choosing a value of ε_x, for example, 0.5×10^{-3}. For the known value of s_{xe}, which is 63 mm (2.5 in.), the values of β and θ are found from Eq. (27) and (28) as 0.280 and 29.4 degrees. With β and θ known, the shear strength *v* and the concrete contribution v_c can then be found from Eq. (18). In this case, where v_s is zero, both *v* and v_c equal 1.293 MPa (187 psi). If the longitudinal steel does not yield, the axial tension f_x, corresponding to the chosen value of ε_x and the resulting values of *v*, v_c, and θ can be determined by rearranging Eq. (1) and (11) and by recalling that f_1 equals $v_c/\cot\theta$. This gives

$$f_x = \rho_x E_s \varepsilon_x - v \cot\theta + v_c / \cot\theta \qquad (31)$$

$$= 0.022 \times 200{,}000 \times 0.5 \times 10^{-3} - 1.293\cot(29.4 \text{ deg})$$

$$+ 1.293/\cot(29.4 \text{ deg}) = 2.200 - 2.293 + 0.729$$

$$= 0.636 \text{ MPa (92 psi)}$$

If the longitudinal steel yields at the crack, however, there is an upper limit to f_x that can be determined by rearranging Eq. (4) and by recalling that v_{ci} equals v_c. This gives

$$f_x \leq \rho_x f_y - (v + v_c)\cot\theta \qquad (32)$$

$$\leq 0.0220 \times 416 - (1.293 + 1.293)\cot(29.4 \text{ deg})$$

$$\leq 9.152 - 4.587 = 4.565 \text{ MPa (662 psi)}$$

Hence, when ε_x at failure equals 0.5×10^{-3}, the failure shear is 1.293 MPa (187 psi) and the axial tension at failure is 0.636 MPa (92 psi). Repeating these calculations for different values of ε_x gives the interaction line labeled "Simplified MCFT" in Fig. 10. This interaction line is concave upward in the region where Eq. (31) governs the magnitude of f_x and is concave down in the region where Eq. (32) governs.

The shear-axial tension interaction diagram predicted for the PB elements by program Membrane-2000 is also shown in Fig. 10. Whereas the MCFT and Simplified MCFT interaction diagrams have very similar shapes, the Simplified MCFT is somewhat more conservative than the MCFT. Both procedures provide conservative estimates of the observed shear strengths of the elements. Also shown in Fig. 10 is the reduction in shear capacity due to axial tension predicted by the ACI approach. For elements without transverse reinforcement, the shear capacity is predicted to be equal to the diagonal cracking load. It can be seen in Fig. 10, however, that this approach greatly overestimates the detrimental effect of tension on shear strengths. This figure also suggests that the ACI approach may overestimate the beneficial effects of compression.[31]

STRENGTH PREDICTIONS FOR 102 REINFORCED CONCRETE ELEMENTS

Table 1 summarizes essentially all of the experimental results[18,20-22,29-30,32-38] available to the authors for reinforced concrete elements loaded in pure shear or shear combined with uniaxial stress (that is, $f_z = 0$). These 102
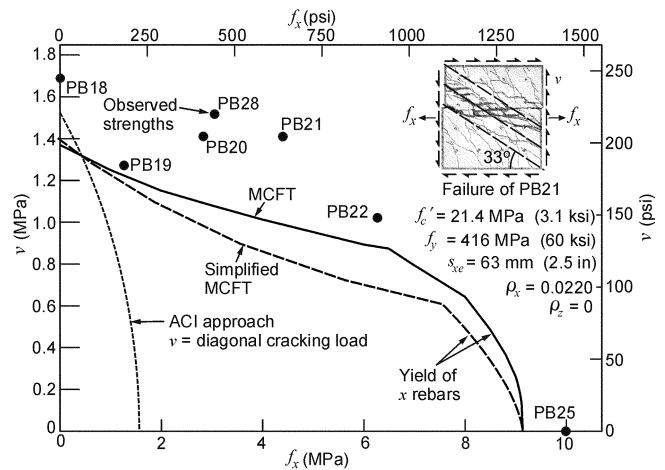
Fig. 10—Tension-shear interaction for elements with no transverse reinforcement.
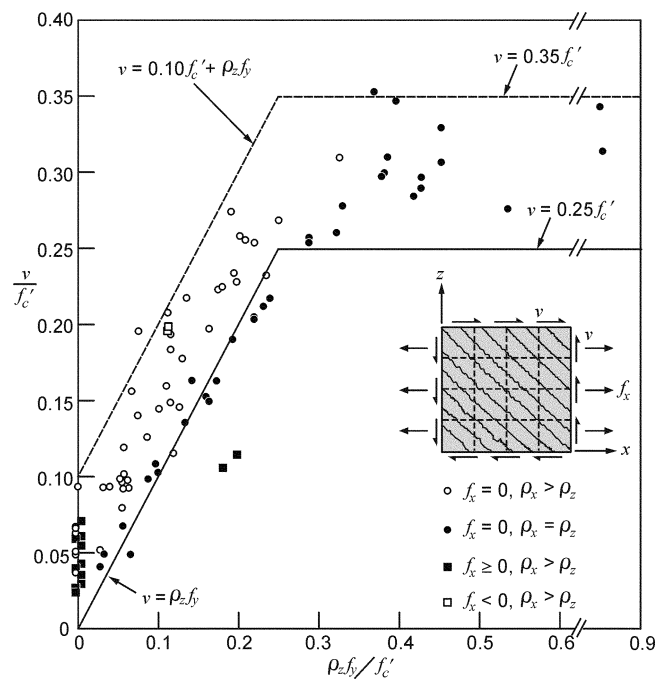
Fig. 11—Influence of amount of transverse reinforcement on shear strength of elements.

elements were loaded using five different testing machines, in four different research laboratories, in three different countries. The test specimens ranged in size from 890 x 890 x 70 mm (35 x 35 x 3 in.) to 2510 x 2510 x 140 mm (99 x 99 x 5.5 in.). Concrete strengths ranged from 14.5 to 102 MPa (2100 to 14,800 psi), whereas the amounts of longitudinal reinforcement varied from 0.18 to 6.39%. Twenty-nine of the elements did not contain any transverse reinforcement and 22 of these were loaded under various combinations of axial tension and shear. The other 73 elements had amounts of from 0.18 to 5.24% of transverse reinforcement, with two of these elements being loaded in combined tension and shear, and two in combined compression and shear.

Figure 11 compares the observed failure shear of the elements with the amount of transverse reinforcement. Recall that the 45-degree truss model predicts that *v* should equal $\rho_z f_y$. For elements containing the same amount of longitudinal and transverse reinforcement, this prediction is

Table 1—Summary of experimental results

Panel	f_c', MPa	ρ_x, %	f_{yx}, MPa	S_x, mm	$\rho_z f_y/f_c'$	f_x/v	V_{exp}/f_c'	Full MCFT	Simp. MCFT	ACI
Vecchio and Collins[18]; a_g = 6 mm										
PV1	34.5	1.79	483	51	0.235	0	0.23	0.93	0.96	1.37
PV2	23.5	0.18	428	51	0.033	0	0.049	1.47	1.41	0.48
PV3	26.6	0.48	662	51	0.120	0	0.115	0.95	0.96	0.63
PV4	26.6	1.03	242	51	0.096	0	0.109	1.12	1.13	0.68
PV5	28.3	0.74	621	102	0.163	0	0.150	0.91	0.92	0.80
PV6	29.8	1.79	266	51	0.159	0	0.153	0.95	0.95	0.84
PV10	14.5	1.79	276	51	0.190	0	0.27	1.06	1.10	1.05
PV11	15.6	1.79	235	51	0.197	0	0.23	0.98	0.98	0.90
PV12	16.0	1.79	469	51	0.075	0	0.196	1.09	1.19	1.24
PV16	21.7	0.74	255	51	0.087	0	0.099	1.12	1.12	0.62
PV18	19.5	1.79	431	51	0.067	0	0.156	1.08	1.08	1.10
PV19	19.0	1.79	458	51	0.112	0	0.21	0.95	1.06	1.10
PV20	19.6	1.79	460	51	0.134	0	0.22	0.93	1.00	1.04
PV21	19.5	1.79	458	51	0.201	0	0.26	0.91	1.03	1.14
PV22	19.6	1.79	458	51	0.327	0	0.31	0.98	1.24	1.38
PV26	21.3	1.79	456	51	0.219	0	0.25	0.88	1.02	1.18
PV27	20.5	1.79	442	51	0.385	0	0.31	0.96	1.24	1.41
PV30	19.1	1.79	437	51	0.249	0	0.27	0.88	1.07	1.18
Bhide and Collins[29,30]; a_g = 9 mm (PB15-27 series with lightweight aggregate)										
PB11	25.9	1.09	433	90	0	0	0.049	1.02	1.03	0.75
PB12	23.1	1.09	433	90	0	0	0.066	1.28	1.30	0.96
PB4	16.4	1.09	423	90	0	1.00	0.071	1.25	1.35	1.40
PB6	17.7	1.09	425	90	0	1.00	0.065	1.28	1.30	1.33
PB7	20.2	1.09	425	90	0	1.90	0.043	0.97	1.05	1.34
PB8	20.4	1.09	425	90	0	3.00	0.039	0.99	1.08	1.74
PB10	24.0	1.09	433	90	0	5.94	0.023	0.92	0.99	2.10
PB13	23.4	1.09	414	90	0	∞	0.201*	1.04	1.06	1.06
PB24	20.4	1.10	407	90	0	∞	0.236*	1.08	1.10	1.10
PB15	38.4	2.02	485	45	0	0	0.051	1.02	1.16	0.95
PB16	41.7	2.02	502	45	0	1.96	0.035	0.98	1.13	1.61
PB14	41.1	2.02	489	45	0	3.01	0.037	1.13	1.34	2.39
PB17	41.6	2.02	502	45	0	5.93	0.029	1.04	1.31	3.47
PB27	37.9	2.02	502	45	0	∞	0.296*	1.11	1.11	1.11
PB18	25.3	2.20	402	45	0	0	0.067	1.06	1.13	1.02
PB19	20.0	2.20	411	45	0	1.01	0.064	0.98	1.09	1.40
PB20	21.7	2.20	424	45	0	2.04	0.065	1.16	1.33	2.25
PB28	22.7	2.20	426	45	0	1.98	0.067	1.23	1.40	2.32
PB21	21.8	2.20	402	45	0	3.08	0.065	1.26	1.46	3.09
PB22	17.6	2.20	433	45	0	6.09	0.059	1.13	1.38	4.62
PB25	20.6	2.20	414	45	0	∞	0.485*	1.10	1.10	1.10
PB29	41.6	2.02	496	45	0	2.02	0.036	1.02	1.15	1.69
PB30	40.04	2.02	496	45	0	2.96	0.037	1.10	1.27	2.29
PB31	43.4	2.02	496	45	0	5.78	0.026	0.97	1.18	3.13
Yamaguchi et al.[28]; a_g = 20 mm										
S-21	19.0	4.28	378	150	0.849	0	0.34	0.89	1.37	1.50
S-31	30.2	4.28	378	150	0.535	0	0.28	0.80	1.10	1.52
S-32	30.8	3.38	381	150	0.418	0	0.26	0.87	1.14	1.58
S-33	31.4	2.58	392	150	0.323	0	0.26	0.86	1.04	1.46
S-34	34.6	1.91	418	150	0.230	0	0.21	0.91	0.92	1.25
S-35	34.6	1.33	370	150	0.142	0	0.163	1.15	1.15	0.97
S-41	38.7	4.28	409	150	0.452	0	0.31	0.95	1.23	1.91
S-42	38.7	4.28	409	150	0.452	0	0.33	1.02	1.32	2.06
S-43	41.0	4.28	409	150	0.427	0	0.29	0.91	1.16	1.86
S-44	41.0	4.28	409	150	0.427	0	0.30	0.94	1.19	1.91
S61	60.7	4.28	409	150	0.288	0	0.25	0.90	1.01	1.98
S-62	60.7	4.28	409	150	0.288	0	0.26	0.91	1.03	2.01
S-81	79.7	4.28	409	150	0.220	0	0.20	0.92	0.92	1.82
S-82	79.7	4.28	409	150	0.220	0	0.20	0.92	0.93	1.83

Table 1 (cont.)—Summary of experimental results

Panel	f_c', MPa	ρ_x, %	f_{yx}, MPa	S_x, mm	$\rho_z f_y/f_c'$	f_x/v	V_{exp}/f_c'	Full MCFT	Simp. MCFT	ACI
Andre[32]; a_g = 9 mm; KP a_g = 20 mm										
TP1	22.1	2.04	450	45	0.208	0	0.26	0.92	1.02	1.21
TP1A	25.6	2.04	450	45	0.179	0	0.22	0.89	0.90	1.14
KP1	25.2	2.04	430	89	0.174	0	0.22	0.89	0.90	1.12
TP2	23.1	2.04	450	45	0.199	3.00	0.114	1.01	1.02	0.72
KP2	24.3	2.04	430	89	0.180	3.00	0.106	1.03	1.06	0.68
TP3	20.8	2.04	450	45	0	3.00	0.061	1.27	1.34	2.75
KP3	21.0	2.04	430	89	0	3.00	0.054	1.15	1.22	2.47
TP4	23.2	2.04	450	45	0.396	0	0.35	1.09	1.39	1.68
TP4A	24.9	2.04	450	45	0.369	0	0.35	1.14	1.41	1.77
KP4	23.0	2.04	430	89	0.381	0	0.30	0.94	1.20	1.44
TP5	20.9	2.04	450	45	0	0	0.093	1.49	1.42	1.28
KP5	20.9	2.04	430	89	0	0	0.063	1.01	0.98	0.87
Kirschner and Khalifa[20,21]; a_g = 10 mm										
SE1	42.5	2.92	492	72	0.110	0	0.159	0.90	0.94	1.04
SE5	25.9	4.50	492	72	0.855	0	0.31	0.89	1.26	1.60
SE6	40.0	2.92	492	72	0.040	0	0.094	0.95	0.99	1.02
Porasz and Beidermann[33,34]; a_g = 10 mm										
SE11	70.8	2.93	478	34	0.063	0	0.093	0.83	0.90	0.91
SE 12	75.9	2.94	450	72	0.060	0	0.098	0.96	1.01	0.99
SE 13	80.5	6.39	509	54	0.115	0	0.149	0.82	0.86	1.34
SE14	60.4	4.48	509	72	0.378	0	0.30	1.03	1.19	2.32
Marti and Mayboom[35]; a_g = 13 mm (constant axial load f_x/v at failure)										
PP1	27	1.95	480	108	0.116	0	0.183	0.98	1.02	1.02
PP2	28.1	1.59	563	108	0.111	−0.38	0.196	1.06	1.08	0.95
PP3	27.7	1.24	684	108	0.113	−0.80	0.199	1.03	1.02	0.86
Vecchio et al.[36,37]; a_g = 10 mm										
PA1	49.9	1.65	606	45	0.086	0	0.126	0.94	1.03	0.95
PA2	43	1.66	606	45	0.100	0	0.145	0.94	1.02	0.96
PHS1	72.2	3.25	606	44	0	0	0.037	1.07	1.08	0.97
PHS2	66.1	3.25	606	44	0.033	0	0.093	1.13	1.25	1.27
PHS3	58.4	3.25	606	44	0.074	0	0.140	0.99	1.13	1.20
PHS8	55.9	3.25	606	44	0.115	0	0.193	1.02	1.15	1.45
PC1	25.1	1.65	500	50	0.163	0	0.197	0.84	0.87	0.99
Pang and Hsu[22]; a_g = 19 mm										
A2	41.3	1.19	463	189	0.134	0	0.136	1.01	1.01	0.87
A3	41.6	1.79	447	189	0.192	0	0.190	0.98	0.99	1.23
A4	42.5	2.98	470	189	0.330	0	0.28	0.97	1.11	1.82
B1	45.2	1.19	463	189	0.056	0	0.092	1.01	1.08	0.87
B2	44.1	1.79	447	189	0.126	0	0.146	0.96	0.96	0.97
B3	44.9	1.79	447	189	0.057	0	0.102	0.94	1.05	0.96
B4	44.8	2.99	470	189	0.057	0	0.119	0.92	1.10	1.12
B5	42.8	2.98	470	189	0.129	0	0.177	0.89	0.96	1.16
B6	42.8	2.98	470	189	0.194	0	0.23	0.95	0.96	1.53
Zhang and Hsu[38]; a_g = 13 mm										
VA1	95.1	1.19	445	94	0.056	0	0.068	1.04	1.20	0.75
VA2	98.2	2.39	409	94	0.100	0	0.103	1.03	1.03	1.02
VA3	94.6	3.59	455	94	0.173	0	0.163	0.94	0.94	1.59
VA4	103.1	5.24	470	94	0.239	0	0.22	1.00	0.91	2.21
VB1	98.2	2.39	409	94	0.054	0	0.080	1.01	1.07	0.91
VB2	97.6	3.59	455	94	0.054	0	0.097	0.95	1.13	1.10
VB3	102.3	5.98	445	94	0.052	0	0.099	0.90	1.08	1.17
VB4	96.9	1.79	455	189	0.027	0	0.052	0.97	1.12	0.85
							Average	1.01	1.11	1.40
							COV	12.2	13.0	46.7

*Tested in pure axial tension, no shear, values are f_x/f_c'.
Note: 1 MPa = 145 psi, 1 mm = 0.03937 in.

very accurate provided that the concrete does not crush prior to yielding of the reinforcement. Such crushing failures are possible for shear stresses above approximately $0.25f_c'$, though failure stresses as high as $0.35f_c'$ have been observed. Elements that have more longitudinal reinforcement than transverse reinforcement (that is, $\rho_x > \rho_z$) fail at shear stresses higher than those predicted by the 45-degree truss model when loaded in pure shear. It is shown in Fig. 11 that the observed shear strengths of these elements can be as high as $\rho_z f_y + 0.10f_c'$. Under combined tension and shear, however, elements with transverse reinforcement can fail at shear stresses as low as $\rho_z f_y - 0.085f_c'$. Given the considerable spread in the observed shear strengths, it is understandable that finding a simple but accurate empirical correction factor to the 45-degree truss model is a difficult task.

The predicted capacities for the elements that result from using the ACI approach of taking the shear strength as the diagonal cracking load plus $\rho_z f_y$ are compared to the experimentally determined failure shear stresses in Table 1. While this approach is simple to apply, it does not give results that are acceptably accurate. Because yielding of the longitudinal reinforcement due to shear is not checked, the approach can be seriously unconservative for elements where ρ_x does not greatly exceed ρ_z (ratios of experimental to predicted failure shear being as low as 0.48). The approach can also be unconservative for elements with transverse reinforcement subjected to axial tension (ratios as low as 0.68). This is because the axial tension can cause θ to be greater than 45 degrees, which makes v_s less than $\rho_z f_y$. On the other hand, the method overestimates the reduction in shear capacity caused by axial tension for members without transverse reinforcement (ratios of experimental to predicted capacities as high as 4.62) and also overestimates the increase in shear capacity caused by axial compression (refer to Specimens PP1 to PP3). Overall, the average value of the experimental to predicted shear stress ratio by the ACI approach is 1.40 and the coefficient of variation (COV) is 46.7%.

Solving the full set of equations of the MCFT to find the predicted shear strength of an element is a complex task that requires a computer program such as Membrane-2000. The ratios of the experimental failure shears to the failure shears predicted by this program are given in Table 1. It can be seen that, while complex, this procedure is very accurate with the average value of the ratio being 1.01 and the COV being only 12.2%. While a little more complex than the ACI calculations, the simplified MCFT calculations can be performed on the "back of an envelope" and yield results that are nearly as accurate as the full version of the MCFT. Thus, the average ratio of experimental-to-predicted failure shear for this method is 1.11 and the COV is 13.0%.

CONCLUSIONS

Understanding the behavior of reinforced concrete subjected to shear is challenging, partly due to the difficulty of performing pure shear tests. Over 100 such tests have been performed during the last 25 years, however, and the results from these tests are summarized in this paper and compared with three different shear theories, including the ACI code.

This paper summarizes the relationships of the MCFT. This theory can model the full load-deformation response of reinforced concrete panels subjected to arbitrary biaxial and shear loading. Solving the equations, however, requires special-purpose computer programs and the method is, thus,

not practical for "back of the envelope" calculations. While complex, the theory is accurate and the average ratio of experimental-to-predicted shear strength of the 102 panels is 1.01 with a COV of only 12.2%.

On many occasions, a full load-deformation analysis is not needed; rather, a quick calculation of shear strength is required. This paper presents a simplified version of the MCFT. At the heart of the method is a simple equation for β and a simple equation for θ. While simple, the method provides excellent predictions of shear strength. The average ratio of experimental-to-predicted shear strength of the simplified MCFT is 1.11 with a COV of 13.0%.

It is hoped that the new simplified method explained in this paper can help others improve their understanding of shear behavior as easily as it has for the authors. In addition, it is hoped that it can help in the development of new codes of practice that could one day become as internationally well accepted for shear design as the plane sections method currently is for flexural design.

REFERENCES

1. ACI Committee 318, "Building Code Requirements for Structural Concrete (ACI 318-05) and Commentary (318R-05)," American Concrete Institute, Farmington Hills, Mich., 2005, 430 pp.

2. AASHTO LRFD, "Bridge Design Specifications and Commentary," 3rd Edition, American Association of State Highway Transportation Officials, Washington, D.C., 2004, 1264 pp.

3. CEN, "BS EN 1992-1-1:2004 Eurocode 2. Design of Concrete Structures. Part 1: General Rules and Rules for Buildings," 2004, 230 pp.

4. CSA Committee A23.3, "Design of Concrete Structures (CSA A23.3-04)," Canadian Standards Association, Mississauga, 2004, 214 pp.

5. JSCE, "Specification for Design and Construction of Concrete Structures: Design, JSCE Standard, Part 1," Japan Society of Civil Engineers, Tokyo, 1986.

6. Vecchio, F. J., and Collins, M. P., "The Modified Compression Field Theory for Reinforced Concrete Elements Subjected to Shear," ACI JOURNAL, *Proceedings* V. 83, No. 2, Mar.-Apr. 1986, pp. 219-231.

7. Vecchio, F. J., "Nonlinear Finite Element Analysis of Reinforced Concrete Membranes," *ACI Structural Journal*, V. 86, No. 1, Jan.-Feb. 1989, pp. 26-35.

8. Wong, P. S.-L., "User Facilities for Two-Dimensional Nonlinear Finite Element Analysis of Reinforced Concrete," MASc thesis, Department of Civil Engineering, University of Toronto, Toronto, Ontario, Canada, 2002, 213 pp.

9. Bentz, E. C., "Sectional Analysis of Reinforced Concrete Members," PhD thesis, Department of Civil Engineering, University of Toronto, Toronto, Ontario, Canada, 2000, 198 pp.

10. Collins, M. P.; Mitchell, D.; Adebar, P.; and Vecchio, F. J., "A General Shear Design Method," *ACI Structural Journal*, V. 93, No. 1, Jan.-Feb. 1996, pp. 36-45.

11. Ritter, W., "Die Bauweise Hennebique (Construction Techniques of Hennebique)," Schweizerische Bauzeitung, Zürich, V. 33, No. 7, Feb. 1899, pp. 59-61.

12. Mörsch, E., "Der Eisenbetonbau (Reinforced Concrete Construction)," Verlag von Konrad Witwer, Stuttgart, Germany, 1922, 460 pp.

13. ACI Committee 318, "Building Code Requirements for Reinforced Concrete (ACI 318-63)," American Concrete Institute, Farmington Hills, Mich., 1963, 163 pp.

14. Nielsen, M. P., *Limit Analysis and Concrete Plasticity*, Prentice Hall, Englewood Cliffs, N.J., 1984, 420 pp.

15. Muttoni, A.; Schwartz, J.; and Thürlimann, B., *Design of Concrete Structures with Stress Fields*, Birkhäuser, Basel, 1997, 143 pp.

16. Mitchell, D., and Collins, M. P., "Diagonal Compression Field Theory—A Rational Model for Structural Concrete in Pure Torsion," ACI JOURNAL, *Proceedings* V. 71, No. 8, Aug. 1974, pp. 396-408.

17. Collins, M. P., "Towards a Rational Theory for RC Members in Shear," *Journal of the Structural Division*, ASCE, V. 104, No. 4, Apr. 1978, pp. 649-666.

18. Vecchio, F. J., and Collins, M. P., "The Response of Reinforced Concrete to In-Plane Shear and Normal Stresses," *Publication* No. 82-03, Department of Civil Engineering, University of Toronto, Toronto, Ontario, Canada, 1982, 332 pp.

19. Collins, M P., and Mitchell, D., *Prestressed Concrete Structures*, Prentice Hall, Englewood Cliffs, N.J., 1991, 766 pp.

20. Kirschner, U., and Collins, M. P., "Investigating the Behaviour of

Reinforced Concrete Shell Elements," *Publication* No. 86-09, Department of Civil Engineering, University of Toronto, Toronto, Ontario, Canada, Sept. 1986, 209 pp.

21. Khalifa, J., "Limit Analysis of Reinforced Concrete Shell Elements," PhD thesis, Department of Civil Engineering, University of Toronto, Toronto, Ontario, Canada, 1986, 312 pp.

22. Pang, X., and Hsu, T. T. C., "Behavior of Reinforced Concrete Membranes in Shear," *ACI Structural Journal*, V. 92, No. 6, Nov.-Dec. 1995, pp. 665-679.

23. Adebar, P. E., and Collins, M. P., "Shear Strength of Members without Transverse Reinforcement," *Canadian Journal of Civil Engineering*, V. 23, No. 1, Feb. 1996, pp. 30-41.

24. Kani, G. N. J., "How Safe Are Our Large Concrete Beams?" ACI JOURNAL, *Proceedings* V. 64, No. 3, Mar. 1967, pp. 128-142.

25. Shioya, T.; Iguro, M.; Nojiri, Y.; Akiyama, H.; and Okada, T., "Shear Strength of Large Reinforced Concrete Beams. Fracture Mechanics: Application to Concrete," *Fracture Mechanics: Application to Concrete*, SP-118, V. C. Li and Z. P. Bažant, eds., American Concrete Institute, Farmington Hills, Mich., 1989, pp. 259-280.

26. Lubell, A.; Sherwood, E.; Bentz, E. C.; and Collins, M. P., "Safe Shear Design of Large, Wide Beams," *Concrete International*, V. 26, No. 1, Jan. 2004, pp. 66-78.

27. Collins, M. P., and Kuchma, D., "How Safe Are Our Large, Lightly Reinforced Concrete Beams, Slabs, and Footings?" *ACI Structural Journal*, V. 96, No. 4, July-Aug. 1999, pp. 482-490.

28. Yamaguchi, T.; Koike, K.; Naganuma, K.; and Takeda, T., "Pure Shear Loading Tests on Reinforced Concrete Panels Part I: Outlines of Tests," *Proceedings*, Japanese Architectural Association, Kanto Japan, Oct. 1988.

29. Bhide, S. B., and Collins, M. P., "Reinforced Concrete Elements in Shear and Tension," *Publication* No. 87-02, Department of Civil Engineering, University of Toronto, Toronto, Ontario, Canada, Jan. 1987, 308 pp.

30. Bhide, S. B., and Collins, M. P., "Influence of Axial Tension on the Shear Capacity of Reinforced Concrete Members," *ACI Structural Journal*, V. 86, No. 5, Sept.-Oct. 1989, pp. 570-581.

31. Gupta, P. R., and Collins, M. P., "Evaluation of Shear Design Procedures for Reinforced Concrete Members under Axial Compression," *ACI Structural Journal*, V. 98, No. 4., July-Aug. 2001, pp. 537-547.

32. Andre, H., "Toronto/Kajima Study on Scale Effects in Reinforced Concrete Elements," MASc thesis, Department of Civil Engineering, University of Toronto, Toronto, Ontario, Canada, 1987, 157 pp.

33. Porasz, A., "An Investigation of the Stress-Strain Characteristics of High Strength Concrete in Shear," MASc thesis, Department of Civil Engineering, University of Toronto, Toronto, Ontario, Canada, 1989, 173 pp.

34. Biedermann, J. D., "The Design of Reinforced Concrete Shell Elements: An Analytical and Experimental Study," MASc thesis, Department of Civil Engineering, University of Toronto, Toronto, Ontario, Canada, 1987, 59 pp.

35. Marti, P., and Meyboom, J., "Response of Prestressed Concrete Elements to In-Plane Shear Forces," *ACI Structural Journal*, V. 89, No. 5, Sept.-Oct. 1992, pp. 503-513.

36. Vecchio, F. J.; Collins, M. P.; and Aspiotis, J., "High-Strength Concrete Elements Subjected to Shear," *ACI Structural Journal*, V. 91, No. 4, July-Aug. 1994, pp. 423-433.

37. Vecchio, F. J., and Chan, C. C. L., "Reinforced Concrete Membrane Elements with Perforations," *Journal of Structural Engineering*, ASCE, V. 116, No. 3, Mar. 1990, pp. 72-78.

38. Zhang, L.-X., and Hsu, T. T. C., "Behavior and Analysis of 100 MPa Concrete Membrane Elements," *Journal of Structural Engineering*, ASCE, V. 124, No. 1, Jan. 1998, pp. 24-34.